Archives of Mechanics • Archiwum Mechaniki Stosowanej • 24, 5–6, pp. 919–930, Warszawa 1972

On the motion of flat landslides and avalanches treated as a problem in plasticity

W. SZCZEPIŃSKI (WARSZAWA)

ON THE BASIS of the mathematical theory of plasticity, theoretical static and kinematic solutions are presented for a layer of granular material, soil or snow sliding down along a rigid surface inclined to the horizontal. These solutions are connected with certain stages of motion of landslides or avalanches and with problems of motion of granular materials in certain industrial handling installations. It is shown that an infinite number of kinematic solutions can be constructed for the local pile-up or rupture of the layer.

W oparciu o matematyczną teorię plastyczności przedstawiono teoretyczne rozwiązania statyczne i kinematyczne dla warstwy ośrodka sypkiego, gruntu lub śniegu zsuwającego się po nachylonym zboczu. Rozwiązania te mają związek z pewnymi etapami ruchu lawin ziemnych lub śnieżnych oraz z ruchem ośrodków sypkich w niektórych urządzeniach przeładunkowych. Wskazano na możliwość zbudowania nieskończenie wielu rozwiązań kinematycznych dla lokalnego spiętrzania się lub rozrywania warstwy.

Исходя из математической теории пластичности, представлены теоретические статические и кинематические решения для задачи о слое сыпучей среды, грунта или снега, сползающем по склону горы под действием собственного веса. Эти решения связаны с некоторыми этапами движения грунтовых или снежных обвалов, а также с движением сыпучей среды в некоторых погрузочных устройствах. Показаны возможности построения бесконечного числа кинематических решений для случаев локального нагромождения или разрывания слоя.

1. Introduction

IN 1951, J. F. NYE published the work [1] in which the flow of glaciers and ice-sheets was treated as a problem in plasticity. In a glacier, a great mass of ice flows plastically under its own weight. It is assumed that the ice behaves as a rigid-ideally plastic body flowing plastically when the shear stress reaches a certain critical constant value.

The same ideally plastic model was later used by H. ZIEGLER [2] for the analysis of the motion of a snow-sheet. Ziegler presented a more rigorous treatment of the problem and gave an analytical solution for the velocity field in the zone of passive flow. W. KUPPER [3] extended the analysis for the material obeying the Coulomb yield criterion and discussed qualitatively velocity fields in zones of local passive or active flow. Results of the two latter works can be directly applied to the analysis of motion of landslides and avalanches flowing down a uniform slope. The solutions referred to are, however, restricted to the particular case of a thick sheet of snow, ice or soil covering the bedrock of a hill, since they are obtained under assumption that the upper layer of the sheet slides downhill along the lower layer of the same material resting motionless on the bed. The surface of velocity discontinuity is identified with the envelope of stress characteristics. This means that if

for an ideally plastic material the slope of the hill is small, or if for the Coulomb material the angle of the slope is only slightly larger than the angle of internal friction, the thickness of the layer should be very large. In the present work we shall show that for smaller values of the thickness local kinematics of another type may be realized.

Various types of such kinematics for a relatively thin layer sliding down a bedrock surface will be presented in Secs. 4, 5 and 6. In Secs. 2 and 3 are discussed in greater detail certain types of velocity fields with several discontinuity lines mentioned in Ref. [3], but without analysis.

In all cases presented below the plane flow is discussed. The Cartesian system of coordinates xy is assumed with the x-axis coinciding with the stress free boundary of the layer

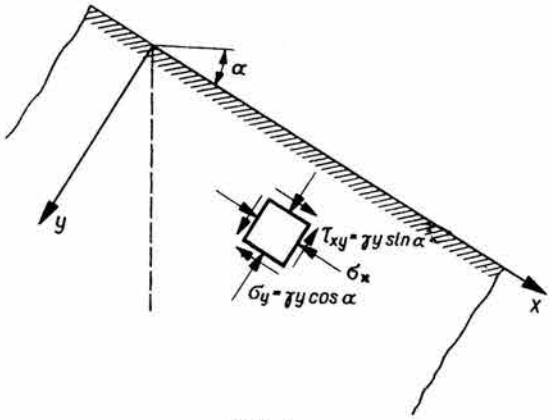

FIG. 1.

and directed downhill (Fig. 1). If compressive stresses are denoted as positive, the equilibrium conditions require the stress components σ_y and τ_{xy} to be equal:

$$\sigma_y = \gamma y \cos\alpha, \qquad \tau_{xy} = \gamma y \sin\alpha, \tag{1.1}$$

where γ is the specific weight of the medium. The third stress component σ_x results from the yield criterion (2.1) or (3.1).

2. Motion of a thick layer of an ideally cohesive medium

Consider first a bulk of a rigid-plastic material obeying the Tresca yield condition

$$(\sigma_x - \sigma_y)^2 + 4\tau_{xy}^2 = 4k^2, \tag{2.1}$$

and bounded by the stress free plane making the angle α with the horizontal. It has been shown in Refs. [1] and [2] that a layer of thickness $h = k/\gamma \sin\alpha$ can slide downhill under its own weight. If the problem is considered in terms of plane flow, the line of velocity discontinuity separating the moving layer from the material at rest coincides with the envelope of stress characteristics. For the sliding layer, an infinite number of kinematically admissible velocity fields can be constructed, the simplest of them consisting in rigid block motion of the entire layer without inner deformation. Two examples of more complex possible modes of deformation which have been treated only marginally in Ref. [3] are discussed below.

Consider a transient region of passive flow in which the sliding velocity of the layer is reduced from the value v_0 to the value v_1 (Fig. 2). Such a reduction of velocity may

result from a local irregularity or non-homogeneity on the sliding surface, causing an impediment to the movement, and is connected with the appearance of the lines of velocity discontinuity passing throughout the layer and forming steps at its surface. Formation of steps at the surface is a well known phenomenon observed in nature. The number of steps formed in the transient zone, or in other words, the number of discontinuity lines appearing, cannot be predicted if an homogeneous material is assumed. For such a model, an arbitrary number of discontinuity lines is kinematically admissible. In real material, local imperfections or slight deviations from homogeneity will cause formation of discontinuities here or there.

In Fig. 2 is presented an example of the solution with two lines of discontinuity AB and DF. The latter is mapped in the velocity plane (Fig. 2b) onto the arc $D'F'$ of a circle

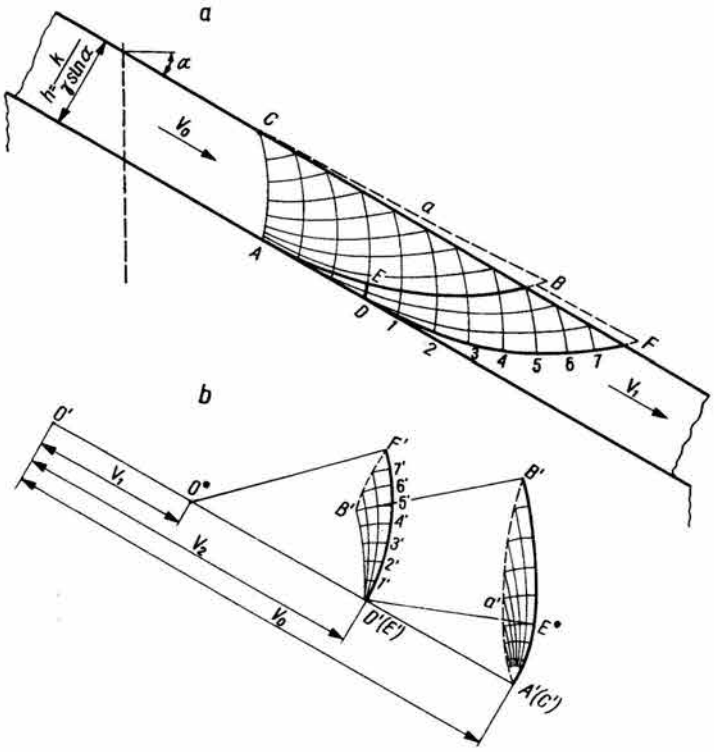

FIG. 2.

of radius O^*D', since the region to the right of DF moves as a rigid body with the velocity v_1. The position of the point D' in the hodograph plane may be chosen arbitrarily. The sector $O'D'$ represents the velocity v_2 of the curvilinear triangle ADE which slides along AD as a rigid body. Thus any value of v_2, $(v_0 > v_2 > v_1)$ may be assumed. Velocities of particles located inside the region $DEBF$ are represented by the corresponding points of the triangle $D'B'F'$ in the hodograph plane. Velocities cannot suffer any jump across DE and, therefore, this sector is represented in the velocity plane by a single point D'. The line AB of velocity discontinuity is mapped onto two arcs $D'B'$ and $A'B^*$. The first of them

results from the velocity solution in $DEBF$. The velocity jump across AB is obviously equal to $[v_0-v_2]$ and at any point must be tangent to this line. This is sufficient to construct the sector $A'B^*$, which is composed of two parts, the sector $A'E^*$ being formed by the arc of a circle of radius $D'A'$. Velocities inside the region ACB can be obtained by constructing in the hodograph plane the mesh of lines orthogonal to the corresponding characteristics. Since AC is not a line of velocity discontinuity, it is represented in the velocity plane by a single point A'. Velocities of particles located on the surface CBF are represented by two separate sectors, $A'a'B^*$ and $B'F'$. Thus two steps are formed at the surface, one at B and the second at F. The rate of internal energy dissipation is everywhere proved positive.

Similar hodographs can be constructed for any arbitrary number of lines of discontinuity. An important particular case is obtained if in the previous solution the velocity v_1 is assumed to be zero. Thus the part of the layer to the right of DF will not move.

As the next example, consider a transient region of active flow in which the thickness of the layer is locally decreasing. Also in this case, a velocity field with two lines of discontinuity FD and BA is analysed (Fig. 3). The layer to the right of AC moves as a rigid

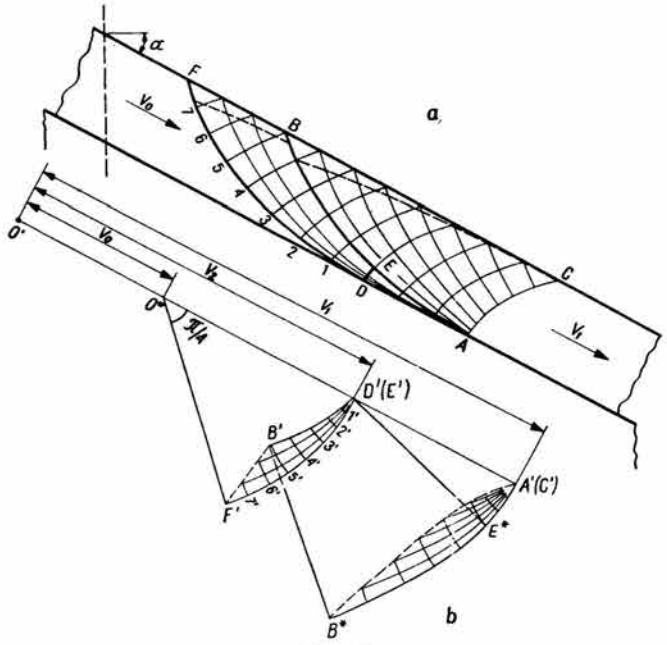

FIG. 3.

body with the velocity v_1, while the sliding velocity of the layer to the left of FD has a smaller value v_0. The curvilinear triangle DEA slides as a rigid body along DA with the velocity v_2, $(v_1 > v_2 > v_0)$. Any value of v_2 in this range may be assumed. Velocities in the region $FDEB$ are represented in the hodograph plane by the corresponding points of the curvilinear triangle $D'B'F'$. Region ACB is mapped onto the region adjacent to $A'E^*B^*$. The mode of deformation of the layer surface is shown by the dashed line in Fig. 3a. Two steps are formed at the surface.

3. Motion of a thick layer of a Coulomb material

For real soils and snow, the Coulomb yield criterion

$$(\sigma_x-\sigma_y)^2+4\tau_{xy}^2 = (\sigma_x+\sigma_y+2H)^2\sin^2\varrho \tag{3.1}$$

is more appropriate than the ideally cohesive model used in the previous section. ϱ is the angle of internal friction and $H = c\tan\varrho$, where c is the cohesion. It has been pointed out in Ref. [3] that velocity fields analogous to the fields described in Sec. 2 can be constructed if the flow rule associated with the Coulomb yield criterion is used. The plastic potential is identified with the yield function and the shearing deformation is accompanied by permanent increase of the volume (dilatancy). The velocity jump across the lines of discontinuity is inclined at the angle of internal friction ϱ to these lines. This means that in our case, if a layer of constant thickness is sliding downhill as a rigid body, the direction of motion is not parallel to the slope. Such a kinematics is obviously unrealistic. Also in other problems of finite flow of soils and granular materials, the use of the flow rule associated with the Coulomb yield condition leads to unrealistic velocity fields. Discussion of that problem and various examples of practical processes of large flow of soils may be found in Refs. [4, 5, 6] together with experimental verification. Much better agreement of experimental and theoretical velocity fields is obtained if the *non-associated* flow rule assuming isotropy and constant volume is used. In this case, for plane flow problems the velocity characteristics are orthogonal, coinciding with the lines of maximum shearing stress. Thus the stress and velocity characteristics are different.

If the Cartesian system of coordinates is assumed as in Fig. 1, the parametric equations of the stress characteristics are (see, for example, Ref. [7])

$$y = \frac{H}{\gamma}\frac{\sin\varrho\sin 2\varphi}{\sin\alpha-\sin\varrho\sin(2\varphi+\alpha)}, \tag{3.2}$$

$$\frac{dx}{d\varphi} = \frac{H}{\gamma}\frac{2\sin\varrho\sin\alpha(\cos 2\varphi-\sin\varrho)}{\tan(\varphi\pm\varepsilon)[\sin\alpha-\sin\varrho\sin(2\varphi+\alpha)]^2},$$

where as the parameter the angle φ, which makes the greater principal stress with the x-axis, was chosen; and $\varepsilon = (\pi/4)-(\varrho/2)$.

For passive flow the boundary condition is $\varphi = 0$ for $y = 0$, and for active flow $\varphi = \pi/2$ for $y = 0$. If $\alpha > \varrho$, the stress characteristics have an envelope parallel to the surface. The equation of the envelope is:

$$y^* = \frac{H}{\gamma}\frac{\sin\varrho}{\sin(\alpha-\varrho)}. \tag{3.3}$$

Velocity characteristics for the non-associated flow rule, which will be used in our considerations, are described by the following parametric equation

$$\frac{dx}{d\varphi} = \frac{H}{\gamma}\frac{2\sin\varrho\sin\alpha(\cos 2\varphi-\sin\varrho)}{\tan\left(\varphi\pm\frac{\pi}{4}\right)[\sin\alpha-\sin\varrho\sin(2\varphi+\alpha)]^2}, \tag{3.4}$$

The second equation coincides with the first of Eqs. (3.2).

For *active flow*, the velocity characteristics have an envelope $y = \bar{y}$ located inside the layer $0 < y < y^*$. The state of stress along the envelope of velocity characteristics is represented by the point A in Fig. 4. From simple geometric considerations, the expression for $\bar{y}$ can be obtained

$$\bar{y} = \frac{H}{\gamma} \frac{\sin\varrho}{\sin\alpha - \cos\alpha \sin\varrho}. \tag{3.5}$$

Thus the envelope of velocity characteristics exists if $\alpha > \arctan(\sin\varrho)$.

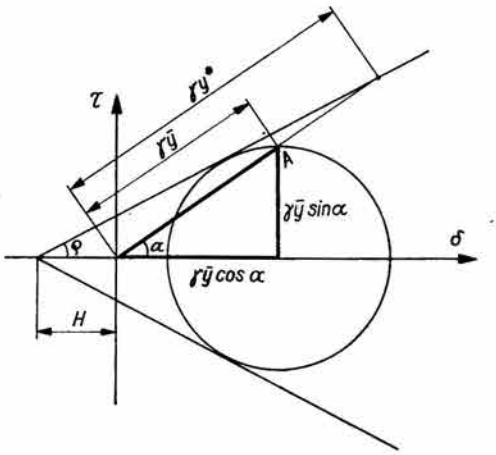

FIG. 4.

If in the entire layer the state of stress is assumed to correspond to the active pressure, sliding downhill along the straight line $y = \bar{y}$ is kinematically admissible. Any local kinematics of the type shown in Fig. 3 forming steps at the surface can also be constructed. The velocity characteristics will now of course have a form slightly different from those for the ideally cohesive material considered in the previous section.

It is interesting to note that for *passive flow* the velocity characteristics have no envelope within the layer $0 < y < y^*$ and, therefore, any kinematics for the non-associated flow rule considered above cannot be constructed. However, construction of a velocity solution for the associated flow rule is in any case possible.

4. Motion of a thin layer of an ideally cohesive medium

Consider a layer of an ideally cohesive medium resting on the slope of a hill. The material of the hill is assumed to be much stronger than that of the layer. We shall discuss here only the case in which the uniform thickness of the layer satisfies the inequality

$$h < k/\gamma \sin\alpha. \tag{4.1}$$

This means that even if the material of the layer is assumed to be in the limit state of stress, the stress characteristics have no envelope within the two bounding lines $y = 0$ and $y = h$. It is obvious that if the angle of friction δ between the layer and the surface of the bed

is smaller than the angle α of the slope, the layer can slide downhill. As in the case considered in Sec. 2, an infinite number of kinematically admissible velocity fields can be constructed including the simple rigid block motion of the entire layer without deformation. Some examples of more elaborate velocity fields are discussed below.

Consider first a transient region of passive flow in which the sliding velocity is reduced from the value v_0 to the value v_1. The simple velocity solution with two lines of discontinuity AB and AC is shown in Fig. 5. To find the velocity jumps across both lines, we decompose the vector of velocity difference $[v_0 - v_1]$ at the point A into the velocity of sliding along AC (vector $O''A'$ in the velocity plane shown in Fig. 5b), and along AB (vector

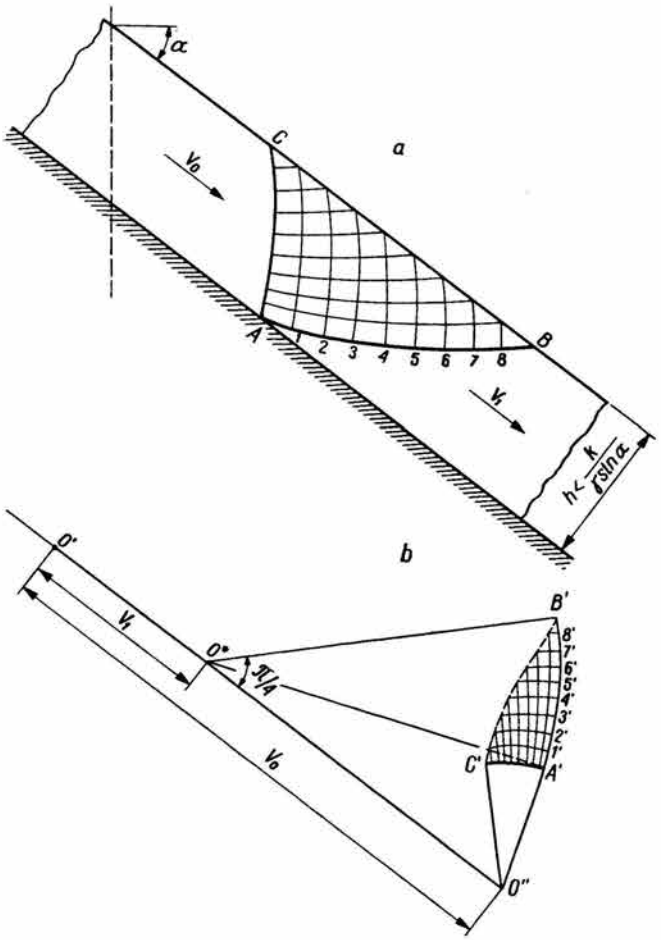

FIG. 5.

O^*A'). The two lines of discontinuity are mapped in the hodograph plane onto the arcs of the circles $A'C'$ and $A'B'$. Velocities at the nodal points of the mesh of characteristics are defined by corresponding nodal points of the network of the hodograph. Two steps are formed at the stress free surface at B and C.

In Fig. 6 is presented another passive flow velocity field with six lines of discontinuity AC, AE, EB, DE, EG and DF. The region ADE slides downhill as a rigid block with the velocity v_2, $(v_0 > v_2 > v_1)$. As in the analogous solution shown in Fig. 2, any value of v_2 in this range can be assumed. Since at the points A and D local kinematics is of the

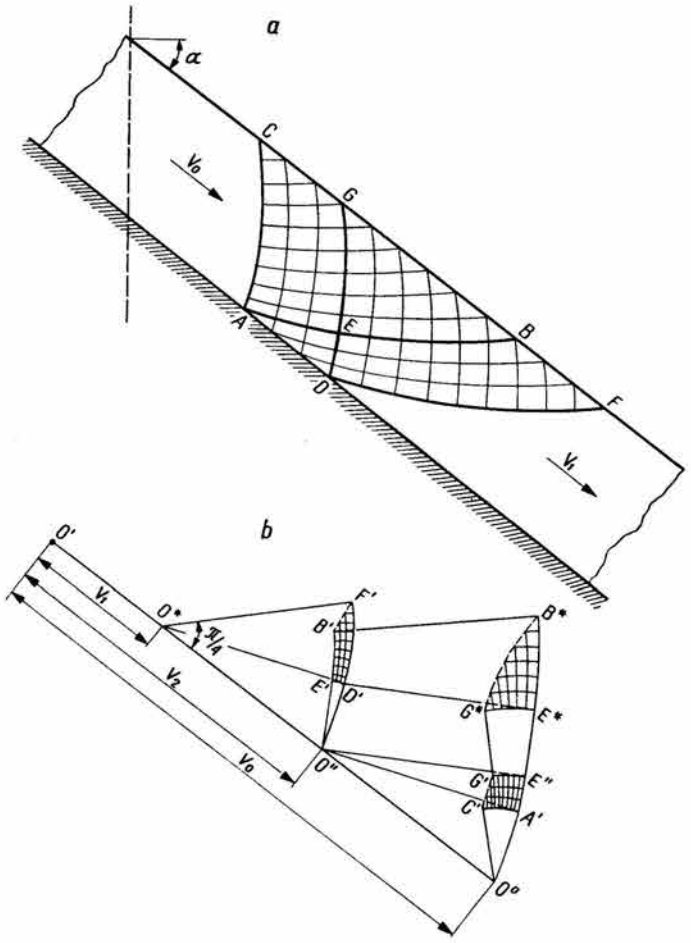

FIG. 6.

same type as the kinematics at the point A in the previous solution, the same procedure can be used for constructing the hodograph. Thus velocities in the regions $AEGC$ and $DEBF$ are represented in the velocity plane by corresponding points of regions $A'E''G'C'$ and $D'E'B'F'$, respectively. Considering compatibility conditions at E, we obtain the velocity jumps across the two remaining discontinuity lines EG and EB. Across the first of these lines, the jump at E is defined by the vector $E''E^*$, and across the second by the vector $E'E^*$. Thus velocities of particles located just above the lines EG and EB are represented by respective points of the curvilinear sectors E^*G^* and E^*B^*. The network of characteristics in EBG is mapped in the velocity plane onto the net covering the curvilinear triangle

$E^*B^*G^*$. Velocities of the stress free boundary are represented by three sectors $B'F'$, B^*G^* $G'C'$. Thus four steps are formed at that surface, at F, B, G and C, as shown in Fig. 7. Each of the three blocks BEG, $CAEG$ and $FDEB$, besides sliding along discontinuity lines undergoes plastic deformation.

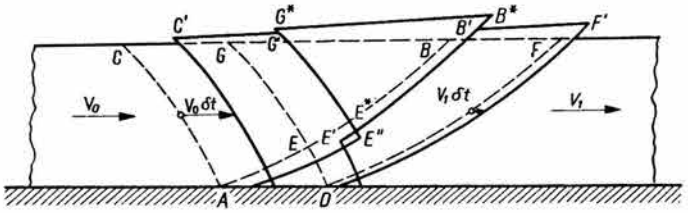

FIG. 7.

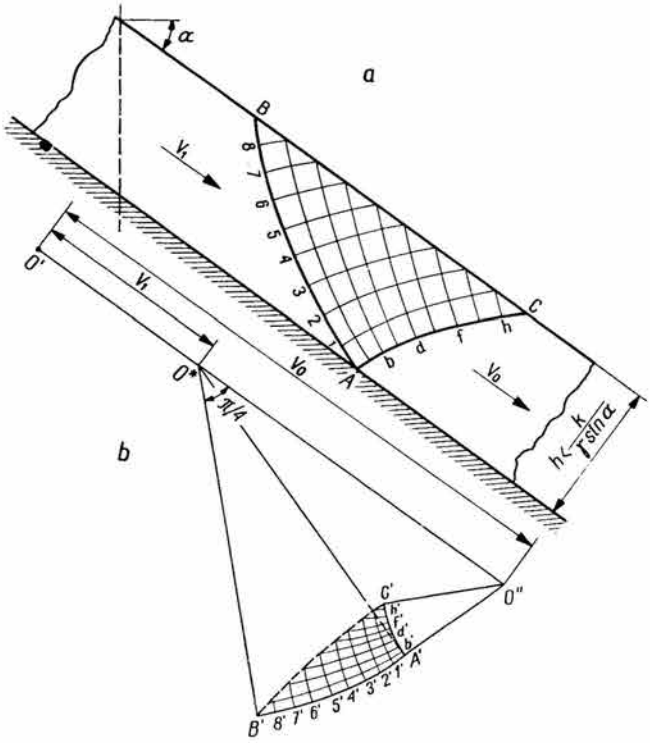

FIG. 8.

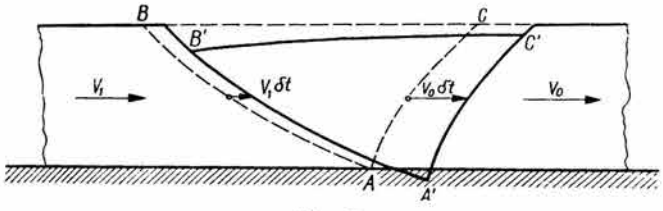

FIG. 9.

In Fig. 8 is presented a simple velocity solution for the zone of active flow. The velocity jumps across the two lines of discontinuity AC and AB are defined from the compatibility conditions at A. The two discontinuity lines are represented in the velocity plane by the arcs $A'C'$ and $A'B'$, respectively. The initial stage of the deformation mode is shown in Fig. 9.

As for the passive flow, also for active flow more elaborate local velocity fields with several lines of discontinuity can be constructed.

5. Motion of a thin layer of a Coulomb material

Velocity fields of the type discussed in Sec. 4 can also be constructed for the Coulomb material by means of the associated or non-associated flow rule. In the present discussion the non-associated rule assuming no dilatancy is used.

Thus for the *passive flow* our present analysis will be restricted to the case of relatively thin layers with the thickness satisfying the inequality

$$h < \frac{H}{\gamma} \frac{\sin\varrho}{\sin(\alpha-\varrho)}, \tag{5.1}$$

or in other words $h < y^*$, where y^* defined by (3.3) is the ordinate of the envelope of stress characteristics. As stated in Sec. 3, the non-associated velocity field has no envelope of velocity characteristics within such a layer.

For the *active flow*, the velocity solution of the type considered in this section and in Sec. 4 can be constructed if the thickness of the layer satisfies the inequality:

$$h < \frac{H}{\gamma} \frac{\sin\varrho}{\sin\alpha - \cos\alpha\sin\varrho}, \tag{5.2}$$

thus if $h < \bar{y}$, where $\bar{y}$ defined by (3.5) is the ordinate of the envelope of velocity characteristics.

In Sec. 3, we have seen that rigid sliding of the entire layer downhill along the envelope of stress or velocity characteristics is possible if $\alpha > \alpha^*$, where $\alpha^* = \varrho$ for the associated flow rule, and $\alpha^* = \arctan(\sin\varrho)$ for the non-associated flow rule under assumption of

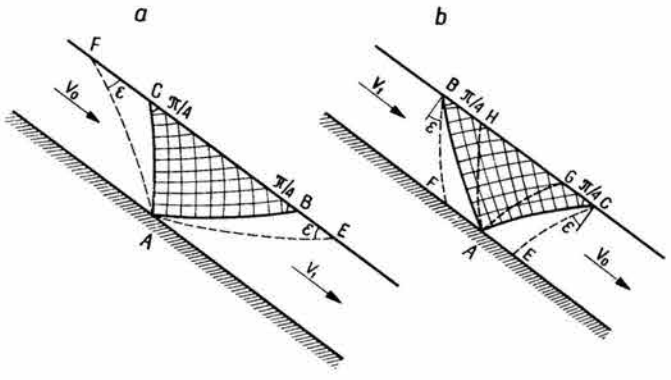

FIG. 10.

the existence of active state of stress in the entire layer. In the case at present under consideration in this section, sliding of the layer along the bedrock surface can occur if the angle of friction δ between that surface and the moving layer satisfies the inequality $\delta < \alpha$.

In Fig. 10 are shown networks of velocity characteristics for simple modes of local flow analogous to those presented in Figs. 5 and 8 for a perfectly cohesive medium.

For the zone of *passive flow* (Fig. 10a), the network of stress characteristics covers the area of the curvilinear triangle AFE. The velocity characteristics can be found by means of Eq. (3.4) and the boundary condition $\varphi = 0$ for $y = 0$. The orthogonal network of velocity characteristics is bounded by the lines AB and AC. Thus the deforming region ACB is for the non-associated flow rule smaller than the region AFE, in which deformation should take place if the associated flow rule was used. The velocity hodograph can be constructed in the same manner as in Fig. 5, starting from the two lines of velocity discontinuity AB and AC. Any of the more elaborate velocity solutions of the type shown in Fig. 6 can also be obtained in the present case.

For the zone of *active flow* (Fig. 10b), the deforming region ABC for the non-associated flow rule is larger than the deforming region AHG predicted by the associated rule. The non-associated orthogonal network of velocity characteristics, shown by continuous lines, has been obtained by integration of Eq. (3.4) with the boundary condition $\varphi = \pi/2$ for $y = 0$. The two bounding velocity characteristics AC and AB represent the lines of velocity discontinuity. The hodograph will be analogous to that shown in Fig. 8.

6. Motion of a layer of a cohesionless medium

The analysis of various modes of motion in the case of cohesionless granular material is very simple, since the stress and velocity characteristics are rectilinear. Thus the local deformation modes consist in rigid block motion. It is obvious that the angle α at which the surface of the layer is inclined to the horizontal must satisfy the inequality $\alpha < \varrho$. The state of stress in the layer is defined by (1.1) and by the expression for σ_x

$$\sigma_x = \gamma y \frac{\cos\alpha(1+\sin^2\varrho) \pm 2\sqrt{\sin^2\varrho - \sin^2\alpha}}{\cos^2\varrho}, \tag{6.1}$$

obtained from the condition of limit state. The upper plus sign corresponds to the case of passive flow, and the lower minus sign to the case of active flow of the medium.

The angle φ_0 which makes the larger principal stress with the x-axis has everywhere the constant value:

$$\varphi_0 = \frac{1}{2}\arctan\frac{\sin\alpha\cos^2\varrho}{\cos\alpha\sin^2\varrho \pm \sqrt{\sin^2\varrho - \sin^2\alpha}}. \tag{6.2}$$

The velocity characteristics for the non-associated flow rule are, therefore, rectilinear making the angle of $\pi/4$ with the direction of the greater principal stress.

It is of interest to note that for the cohesionless material any motion of the types described in Sections 2 and 3 is impossible. By contrast, any solution of the types described in Secs. 4 and 5 is now possible for the arbitrary thickness of the layer.

As an example, the simple velocity solution for the passive flow analogous to that shown in Fig. 5 is presented in Fig. 11. Consider the motion of the region bounded by the lines of velocity discontinuity AB and AC coinciding with the velocity characteristics. Assume the part of the layer to the right of AB to remain at rest, while the part to the left of AC

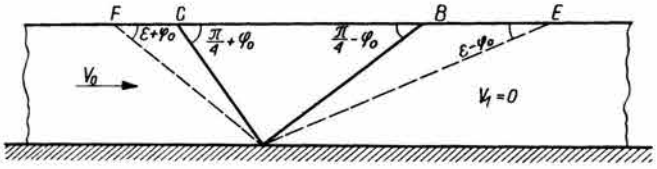

FIG. 11.

moves with velocity v_0. Considering compatibility conditions at A, we find that the triangle ABC has to move as a rigid block with velocity $v_1 = v_0 \cos\left(\frac{\pi}{4} - \varphi_0\right)$ along AB.

In the same manner, more elaborate velocity fields with several lines of discontinuity can be constructed for both the active and passive flows of the layer of granular material.

References

1. J. F. NYE, *The flow of glaciers and ice-sheets as a problem in plasticity*, Proc. Roy. Soc. of London, **207**, 554–572, 1951.
2. H. ZIEGLER, *Methoden der Plastizitätstheorie in der Schneemechanik*, Zeitschr. angew. Math. Physik, **14**, 713–737, 1963.
3. W. KUPPER, *Der plastische Grenzzustand in der schiefen ebenen Erd- oder Schneeschicht*, Zeitschr. Math. Physik, **18**, 705–735, 1967.
4. A. DRESCHER, K. KWASZCZYŃSKA, Z. MRÓZ, *Statics and kinematics of the granular medium in the case of wedge indentation*, Arch. Mech. Stos., **19**, 99–113, 1967.
5. W. SZCZEPIŃSKI, *Some slip-line solutions for earthmoving processes*, Arch. Mech. Stos., **23**, 885–896, 1971.
6. W. SZCZEPIŃSKI, H. WINEK, *On some practical problems of large flow of soils*, Proc. Polish-French Symp. on Rheology, Jabłonna 1971.
7. V. V. SOKOLOVSKY, *Statics of soil media*, Butterworths, London 1960.

INSTITUTE OF FUNDAMENTAL TECHNICAL RESEARCH
POLISH ACADEMY OF SCIENCES

Received May 29, 1972